


RESEARCH

Open Access



Characterization of the coding gain for M-PSK with conjoint signals under correlated Nakagami-m fading channels

Edwin Omosa^{1*} , Peter Akuon^{1†}, Hongjun Xu^{2†} and Vitalis Oduol^{1†}

[†]P. Akuon, H. Xu and V. Oduol have equally contributed to this work.

*Correspondence: edwinomosa@gmail.com

¹ Electrical and Information Engineering, University of Nairobi, 30197-00100 Nairobi, Kenya

² School of Engineering, University of KwaZulu-Natal, Durban X54001-4000, South Africa

Abstract

In the paper, a comprehensive analysis is presented on the conjoint coding gain achieved in arbitrarily correlated M-ary phase-shift keying (M-PSK) signals in a spatial diversity system. The system operates over Nakagami-m fading channels and is affected by additive white Gaussian noise (AWGN). The proposed signal synthesizer primarily induces an even phase shift in the output signals. To enhance the coding gain, an orthogonal transformation matrix is introduced, which effectively preserves energy and operates independently of the channel correlation matrix, making it blind to signal information measurements. The main objective is to generate additional copies of conjoint signals from the received signals, simulating the scenario as if there were more antennas deployed. To evaluate the system's performance in terms of symbol error rate (SER), an analytical framework is developed and its accuracy is validated through Monte-Carlo simulations. Moreover, extensive tests are conducted to explore the impact of different antenna configurations and fading severity levels. The fading severity, denoted as 'm', is varied in the experiments, considering values of 0.5, 1, 3, and 7. Additionally, the measurements incorporate varying antenna spacing values relative to the signal carrier wavelength, specifically 0.1, 0.2, and 0.5. The results obtained from the experiments demonstrate that the coding gains achieved depend on the value of 'm', with higher gains observed for lower 'm' values. However, as 'm' increases, the coding gains become negligible.

Keywords: Virtual receive diversity decorrelator, Conjoint signals, Symbol error rate

Introduction

The presence of correlation among antenna branches in multi-antenna systems negatively affects signal reception, especially in modern compact wireless hand-held devices where antenna spacing is limited. Existing literature assumes independent antenna branches, but in reality, closely spaced antennas are often correlated [1–8]. Hence, it is crucial to tackle the consequences of unwanted correlations between antenna branches. A preferred approach would involve incorporating a decorrelator at the receiver [6–9].

There are various methods available for decorrelation, and one such technique is eigenvalue decomposition (EVD) [2, 10, 11]. EVD can be employed to decompose a covariance matrix of correlated received signals or channels. When EVD is applied

to the covariance matrix, it transforms into a set of mutually orthogonal eigenvectors with dimensions devoid of correlation. Another method for decorrelation is the principal component analysis (PCA). PCA reduces data dimensionality and is grounded in the EVD [12] and [13]. It uses the principal components/eigenvectors from the covariance matrix to obtain decorrelated representations while retaining the variance of the original data.

Due to various limitations such as hardware constraints, space restrictions, and cost factors, it may not always be practical to deploy multiple physical antennas. However, virtual diversity decorrelators, also referred to as virtual antenna arrays or blind decorrelators, provide an alternative solution by simulating the advantages of multiple physical antennas using just one or a few physical antennas [5, 12, 14–16]. These methods remain an active and evolving focus of research and development in the wireless communications field. For instance, previous studies have explored decorrelation receivers, with the Karhunen-Loeve Transformation (KLT) to enhance performance through generating independent virtual antennas [2, 17, 18]. However, the KLT approach requires perfect knowledge of the covariance matrix, which relies on accurate channel state information (CSI) that is often unavailable in practical scenarios.

Furthermore, discrete Fourier transform (DFT) and fast Fourier transform (FFT) techniques have been employed to implement blind decorrelators in wireless communications [19] and [20]. However, a challenge persists in mitigating signal errors caused by correlation. In addition, DFT and FFT may necessitate specific designs, such as uniform circular arrays (UCAs) with uniform circular receive antenna spacing. Despite utilizing the current invention, these approaches yield limited decorrelation gains.

A dual diversity decorrelator that achieves decorrelation by adding and subtracting the received signals from correlated branches, proving effective in dual Selection Combining (SC) and Switch and Stay Combining (SSC) branches has been used in [21]. However, it does not improve equal gain combining (EGC) and square law combining (SLC) techniques [18].

Newly developed techniques have emerged that bypass the need for calculating covariance matrices by updating estimates for individual input training vectors [5]. However, these methods exhibit certain drawbacks in terms of convergence and stability. They may also not be essential for achieving coding gains. This research seeks to illustrate that coding gains can be achieved using a transformation matrix that synthesizes excess virtual signals from received correlated signals under arbitrarily correlated Nakagami-m fading channels with EGC. The essential statistical equations that are simple and converge rapidly, such as the SER and the coding gains, are derived. Analytical and simulation approaches support the obtained results. Furthermore, the effectiveness of the investigated decorrelator is confirmed to approach maximum-ratio combining (MRC), showcasing its superior performance compared to existing approaches.

The motivation for conducting this study stems from [18] and [21], which collectively indicate that no discernible benefits have been observed regarding the de-correlation of signals through EGC combining. [18] and [21] also limit themselves to dual correlated

antenna branches. In contrast, this study will provide empirical evidence to demonstrate that the practice of de-correlating N_r antenna branches through EGC combining does, in fact, yield tangible benefits. Subsequently, the following paragraphs outline the accomplishments in this article:

1. Firstly, we derive the coding gains ((21)) for the EGC combining scheme in arbitrarily correlated M-PSK cojoint signals under Nakagami- m fading channels. To do so, the signal-to-noise ratio (SNR) at the output of the combiner and the SNR at the output of the decorrelator are analysed and used to evaluate the gain of the decorrelator system.
2. Secondly, we show that the coding gains for the EGC combiner in arbitrarily correlated fading channels that follows a Nakagami- m distribution depends on the fading parameter, m .
3. Thirdly, we show that the proposed decorrelator achieves decorrelation. In addition, it is blind, thus simple because it does not estimate the correlation matrix, but depends on the coding gains inherent in the conjoint signals, which are synthesized from the received signals.
4. Finally, we demonstrate that the SER performance of EGC equals the performance of MRC after decorrelation.

The following text describes the structure of this document. The first part serves as an introduction. The second part discusses the modeling of the system. Section three elaborates on signal combining and the resulting SNR. The fourth section examines the performance of the system. A summary of the findings is presented in the fifth section, and the work concludes in the sixth section.

In this study, the symbols used can be explained as follows: Matrices are denoted by bold uppercase letters, scalar quantities are represented by regular letters, and bold lowercase letters represent vectors. The Q-function with a Gaussian distribution is denoted as $Q(\cdot)$. Furthermore, the operators $E[\cdot]$, $(\cdot)^*$, and $(\cdot)^H$ represent the expectation, complex conjugate, and Hermitian operators, respectively. The gamma function is denoted as $\Gamma(\cdot)$, and $J_0(\cdot)$ represents the Bessel function of the first kind with zero order.

Conjoint diversity system modeling

Synthesizer operation and signal combining

A Single-Input Multiple-Output (SIMO) diversity system with N_r receive branches is examined. To process the received signals, a diversity decorrelator is employed, which generates multiple copies of the received signals. These newly generated signals are then fed into a diversity combiner to obtain an approximate version of the transmitted symbol. In the case of N_r diversity branches, N_r signals from the receive antennas produce $N_r(N_r - 1)$ additional decorrelated signals. This results in a total of N_r^2 input signals to the diversity combiner. For instance, if we have 4 receive antennas as shown in Fig. 1, where $N_r = 4$, there will be 12 additional decorrelated outputs. To generate these decorrelated signals, a combination of sum, difference, and conjugate operations is performed

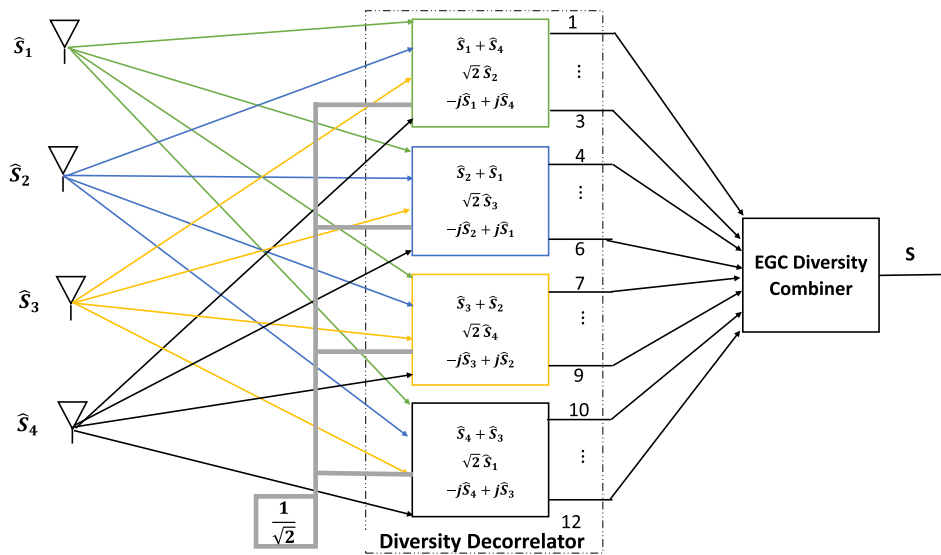


Fig. 1 Decorrelation synthesizer system with $N_r = 4, \theta = 45^\circ$

on selected pairs of signals. This process introduces coding gains rather than diversity gains because the variances of the sum signal $(\hat{s}_i + \hat{s}_k)$, difference signal $(j\hat{s}_k - j\hat{s}_i)$, and branch signal (\hat{s}_i) differ from those of the received branch signals. However, due to some correlation between the sum and difference signals, the resulting decorrelated outputs, known as conjoint signals, are not entirely mutually independent. Finally, the N_r^2 outputs are combined using EGC diversity combiner.

Diversity synthesizer analysis

The suggested diversity decorrelator is presented as,

$$\mathbf{Q}^H = \begin{pmatrix} \cos\theta & \cos\theta \\ -j\sin\theta & j\sin\theta \end{pmatrix} \tag{1}$$

where $\theta = 45^\circ$

Consider z_k as the symbol that has been transmitted. In the case of a receive system with inputs $\hat{\mathbf{s}}$, the de-correlator produces an output $\mathbf{y} = \mathbf{Q}^H \hat{\mathbf{s}}$. When we examine a two-branch system with two inputs, \hat{s}_1 and \hat{s}_2 , the signal at the decorrelator’s output can be expressed as,

$$\begin{pmatrix} y_3 \\ y_4 \end{pmatrix} = \begin{pmatrix} \cos\theta & \cos\theta \\ -j\sin\theta & j\sin\theta \end{pmatrix} \begin{pmatrix} \hat{s}_1 \\ \hat{s}_2 \end{pmatrix} \tag{2}$$

Correlated signal model

The signal received at the i_{th} branch, which is independent, is expressed as,

$$s_i = \alpha_i A_k e^{j\psi_i} e^{j\phi_k} + n_i, \quad i = 1, 2, \dots, N_r \tag{3}$$

where the transmitted signal amplitude and phase angle are denoted by A_k and ϕ_k , respectively. The dependence on the index k can be eliminated for symbol-by-symbol

detection. n_i signifies the AWGN. The phase of the channel, denoted by ψ_i , follows a uniform distribution over the interval $[0, 2\pi]$ for M-PSK during a single signal interval. Additionally, α_i refers to the Nakagami- m fading envelope, which has a probability distribution function for a statistically independent and identically distributed fading channel, as expressed in [22, 23], which is given as,

$$P_\alpha(\alpha) = 2\left(\frac{m}{\Omega}\right)^m \frac{\alpha^{2m-1}}{\Gamma(m)} \exp\left(-\frac{m\alpha^2}{\Omega}\right), \alpha \geq 0 \tag{4}$$

The severity of fading, determined by the parameter m , varies from 0.5 to ∞ . $\Omega = E(\alpha^2)$ represents the average power or the mean squared value of α . The Gamma function, represented by the symbol $\Gamma(m)$, is defined as [9]; $\Gamma(m) = \int_0^\infty y^{m-1} \exp(-y) dy$.

Additionally, the signal received from a correlated Nakagami- m channel, characterized by the correlation coefficient ρ , is expressed as follows.

$$\hat{s}_i = (I_i + jD_i).e^{j\varphi_k} + n_i, i = 1, 2, \dots, N_r \tag{5}$$

where I_i and D_i are random variables that conform to a Gaussian distribution, exhibiting a zero mean and a variance of σ^2 with $E[I_i D_k] = 0 \quad i, k = 1, 2, \dots, N_r$, $C_{I_i I_k} = E[I_i I_k] = \rho\sigma^2$ and $C_{D_i D_k} = E[D_i D_k] = \rho\sigma^2$.

Due to the independence of the noise components and lack of correlation with the signals, $E[n_i n_k] = E[n_i I_k] = E[n_i D_k] = 0$.

The correlation coefficient ρ_{kl} can be used to express the spatial correlation between two received signals from any two branches [24] and [25] as,

$$\rho_{kl} = \frac{E[\hat{h}_k \hat{h}_l^*]}{\sqrt{\sigma_{\hat{h}_k}^2 \sigma_{\hat{h}_l}^2}}, l, k = 1, 2, \dots, N_r \tag{6}$$

The random variables \hat{h}_k and \hat{h}_l , with variances of $\sigma_{\hat{h}_k}^2$ and $\sigma_{\hat{h}_l}^2$ respectively, are included. If \mathbf{R} is a correlation matrix that has been normalized, it can be expressed as [24] [26]:

$$\mathbf{R} = \begin{pmatrix} 1 & \rho_{12} & \dots & \rho_{1N_r} \\ \rho_{21} & 1 & \dots & \rho_{2N_r} \\ \vdots & \vdots & \ddots & \vdots \\ \rho_{N_r} & \dots & \dots & 1 \end{pmatrix} \tag{7}$$

Based on the explanations provided in (6), it is clear that the correlation coefficients $\rho_{k,l}$ and $\rho_{l,k}$ are complex conjugates, meaning $\rho_{k,l} = \rho_{l,k}^*$. Consequently, the correlation matrix, when normalized, exhibits Hermitian properties, implying that it is equal to its conjugate transpose ($\mathbf{R}^H = \mathbf{R}$).

The process of eigenvalue decomposition (EVD) can be employed to decompose \mathbf{R} into orthogonal eigenvectors and eigenvalues. This decomposition can be achieved through an eigen-filter operation, as explained in [2, 26–30] as,

$$\begin{aligned} \Lambda &= \mathbf{QRQ}^H \\ \mathbf{R} &= \mathbf{Q}^H \Lambda \mathbf{Q} \end{aligned} \tag{8}$$

The matrix \mathbf{Q} consists of orthonormal eigenvectors, and the matrix $\mathbf{\Lambda}$ contains positive eigenvalues. When the EVD is applied, \mathbf{Q} is obtained, and its rows represent orthonormal basis elements, making \mathbf{Q} a unitary transformation. Additionally, $\mathbf{Q}^H = \mathbf{Q}^{-1}$. \mathbf{Q} creates a reciprocal network, and therefore, it is the designed eigen-filter/diversity decorrelator that modifies the input in a unitary manner to produce an output. The functioning of this filter is thoroughly analyzed in reference [24, 27]. Referring to the output of the i_{th} branch, the equivalent channel coefficient is expressed as:

$$\hat{h}_i = \sqrt{\epsilon_i} \hat{\mathbf{Q}}_i \hat{\mathbf{Q}}_i = \sqrt{\epsilon_i} \hat{\mathbf{Q}}_i \hat{\mathbf{h}} \tag{9}$$

where $\epsilon_i \in \mathbf{\Lambda}$ and $\hat{\mathbf{Q}}_i$ refers to the i_{th} column of $\hat{\mathbf{Q}}$. $\hat{\mathbf{h}}_i$ represents an approximation of the correlated Nakagami- m fading channel, which is characterized by a complex channel coefficient. The phase, on the other hand, is uniformly distributed random variable between $(0, 2\pi)$ for M-PSK.

According to [19], the product $(\hat{\mathbf{Q}}_i \hat{\mathbf{h}})$ has entries that are independent of each other. As a result, the correlated paths can be treated as separate branches that have been scaled by eigenvalues. The matrix \mathbf{Q} is typically computed from matrix \mathbf{R} or given. Thus, \mathbf{Q} can be determined without measuring \mathbf{R} , making \mathbf{Q} blind while \mathbf{R} does not need to be measured.

Combiner average output SNR

The expression for the probability density function (PDF) of the instantaneous branch SNR for independent signals in channels that undergo fading, as described by the Nakagami- m model, can be stated as

$$f_{\gamma_k}(\gamma_k) = \left(\frac{m}{\bar{\gamma}_k}\right)^m \frac{\gamma_k^{m-1}}{\Gamma(m)} \exp\left(-\frac{m\gamma_k}{\bar{\gamma}_k}\right), \gamma_k \geq 0 \tag{10}$$

where $\gamma_k = \alpha_k^2 \frac{E_s}{N_{0k}}$

The SNR, $\bar{\gamma}_{k,s}$, of the channel described in Eq. (9) can be depicted as;

$$\bar{\gamma}_{k,s} = \epsilon_k E\{\gamma_k\} = \epsilon_k E\left[\alpha_k^2 \frac{E_s}{N_{0k}}\right] = \epsilon_k \bar{\gamma}_{0,c} \tag{11}$$

The average output SNR, denoted as $\bar{\gamma}_{0,c}$, is calculated to determine the SNR of the combiner’s output. By utilizing the diversity decorrelator, the power distribution of the branch signals is adjusted. Consequently, the output SNRs from the decorrelator, represented as $(\hat{\gamma}_1 \hat{\gamma}_2 \dots \hat{\gamma}_{N_r})$, contain eigenvalues that are scaled in proportion to the average output SNR ($\bar{\gamma}_{0,c}$) of the particular c_{th} combiner in use. Thus,

$$\hat{\gamma}_{k,c} = \epsilon_k \bar{\gamma}_{0,c} \tag{12}$$

We can express the average output SNR using the individual signals from each branch for MRC and EGC as $\bar{\gamma}_{0,c} = \sum_{k=1}^{N_r} \hat{\gamma}_k$. Moreover, as indicated by Eq. (12), we can express the PDF of the SNR for each branch after passing through the decorrelator as

$$f_{\bar{\gamma}_0}(\gamma_k) = \left(\frac{m}{\widehat{\gamma}_{k,c}} \right)^m \frac{\gamma_k^{m-1}}{\Gamma(m)} \exp\left(-\frac{m\gamma_k}{\widehat{\gamma}_{k,c}}\right), \gamma_k \geq 0 \tag{13}$$

This represents the SNR of the correlated system.

Synthesizer gains for EGC

Maximum-ratio combining

The average output SNR for MRC, $\bar{\gamma}_{0,MRC} = \sum_{k=1}^{N_r} \bar{\gamma}_k = N_r \bar{\gamma}_k$ is given in [4, 31, 32], where $\bar{\gamma}_k$ is the average SNR of the output signal at the k_{th} branch and is optimal.

Average SNR approximation for equal-gain combining (EGC)

Given independent fading paths and a total of N_r receive antennas, and considering the symbol received at the i_{th} antenna, r_i , the i_{th} received symbol obtained at the output of the EGC combiner can be expressed as follows:

$$\hat{r}_i = \sum_{i=1}^{N_r} r_i \tag{14}$$

$r_i = \alpha_i \sqrt{E_s} + n_i$ and α_i is the stochastic amplitude of the symbol on the i_{th} path of the i_{th} antenna. E_s represent the symbol energy, and n_i is the AWGN component at the receiver, with a mean of zero and variance $\sigma^2 = N_0/2$ [33].

The conditional SNR per symbol, $\gamma_{0,EGC}$, at the output of the EGC combiner can be calculated according to [5] when symbols are transmitted with equal power as:

$$\gamma_{0,EGC} = \frac{\left(\sum_{i=1}^{N_r} \alpha_i\right)^2 E_s}{\sum_{i=1}^{N_r} N_i} \tag{15}$$

Where N_i denotes AWGN that has been added to the signal and has a power spectral density.

The SNR of the output signal in EGC, $\bar{\gamma}_{0,EGC}$, which is calculated as an average and expressed as the expectation of (15), is determined for the uncorrelated channels with identical power spectral density of AWGN (N_0) as follows [1]:

$$\bar{\gamma}_{0,EGC} = \frac{E_s}{N_r N_0} \left[\sum_{i=1}^{N_r} E\{|\alpha_i|^2\} + \sum_{i=1}^{N_r} \sum_{j \neq i}^{N_r} E(\alpha_i)E(\alpha_j) \right] \tag{16}$$

The expression for $E[\hat{r}^2]$, where $r_i = \alpha_i \sqrt{E_s} + n_i$ represents the i_{th} symbol received at the i_{th} antenna and $r_j = \alpha_j \sqrt{E_s} + n_j$ represents the j_{th} symbol received at the j_{th} antenna (with the superscript removed for simplicity), can be written as:

$$E[\hat{r}^2] = \sum_{i=1}^{N_r} \sum_{j=1}^{N_r} E(r_i r_j) = \sum_{i=1}^{N_r} \sum_{j=1}^{N_r} E\left(\alpha_i \alpha_j E_s + \alpha_i \sqrt{E_s} n_j + \alpha_j \sqrt{E_s} n_i + n_i n_j\right) \tag{17}$$

The aim is to come up with a method that can blindly estimate the SNR without the requirement of transmitting pre-known training symbols. Consequently, we devise a SNR estimator that relies on the symbols received. Given that α follows a Nakagami- m distribution and considering the value of $E[\alpha^k] = \frac{\Gamma(m+\frac{k}{2})}{m^{k/2}\Gamma(m)}$, we can infer that $E[\alpha^2] = \Omega = 1$ and the expected value of $E[\alpha] = \frac{\Gamma(m+\frac{1}{2})}{\sqrt{m}\Gamma(m)}$.

Using (17), it can be shown that Eq. (16) can be expressed as

$$\bar{\gamma}_{0,EGC} = \left[1 + (N_r - 1) \frac{\Gamma^2\left(m + \frac{1}{2}\right)}{m\Gamma^2(m)} \right] \bar{\gamma} \tag{18}$$

where $\bar{\gamma}$ is the average SNR in the different diversity branches.

Decorrelation gain for EGC

In a two-branch system, the synthesizer generates four outputs. To calculate the variance of these outputs, [5] can be used, and the average SNR at the output of the EGC combiner can be expressed as

$$\bar{\gamma}_{0,S} = \frac{N_r([1 + \rho] + [1 - \rho] + 1 + 1)\bar{\gamma}}{4} = N_r\bar{\gamma} \tag{19}$$

The coefficient ρ represents the correlation between two random variables, with its range falling between 0 and 1. Consequently, the gains obtained from de-correlation is given as

$$G_{\bar{\gamma}}(EGC) = \frac{N_r\bar{\gamma}}{\left[1 + (N_r - 1) \frac{\Gamma^2\left(m+\frac{1}{2}\right)}{m\Gamma^2(m)} \right] \bar{\gamma}} = \frac{N_r}{\left[1 + (N_r - 1) \frac{\Gamma^2\left(m+\frac{1}{2}\right)}{m\Gamma^2(m)} \right]} \tag{20}$$

As the synthesizer has to perform its operation on two branches at any given instance, then $N_r = 2$.

$$G_{\bar{\gamma}}(EGC) = \frac{2}{\left[1 + \frac{\Gamma^2\left(m+\frac{1}{2}\right)}{m\Gamma^2(m)} \right]} \tag{21}$$

New combiner output SNR

To calculate the average output SNR of the new combiner, we replace $\hat{\gamma}_{k,c}$ with an expression that incorporates the average SNR of the received branch, $\bar{\gamma}$. By using Eqs. (12) and (18), we obtain

$$\widehat{\gamma}_{k,EGC} = G_{\bar{\gamma}}(EGC) \epsilon_k \frac{\bar{\gamma}_{0,EGC}}{N_r} = G_{\bar{\gamma}}(EGC) \epsilon_k \left(\frac{1 + (N_r - 1) \frac{\Gamma^2(m + \frac{1}{2})}{m\Gamma^2(m)}}{N_r} \right) \bar{\gamma} \quad (22)$$

Similarly, the MRC average output SNR for each correlated branch can be expressed as

$$\widehat{\gamma}_{k,MRC} = \epsilon_k \frac{\bar{\gamma}_{0,MRC}}{N_r} = \epsilon_k \bar{\gamma} \quad (23)$$

An overall formula can be obtained to describe the MRC and EGC combiners by taking into account the average signal-to-noise ratio of each branch. We can merge Eqs. (22) and (23) as

$$\bar{\gamma}_{0,c} = \epsilon_k \beta_c \bar{\gamma} \quad (24)$$

Where

$$\beta_c = \begin{cases} \beta_{MRC} = 1 \text{ for MRC} \\ \beta_{EGC} = \frac{1 + (N_r - 1) \frac{\Gamma^2(m + \frac{1}{2})}{m\Gamma^2(m)}}{N_r} \text{ for EGC} \end{cases}$$

Performance analysis of SER for MPSK under the synthesizer system with correlation

The SER analysis, caused by the fading channel, can be evaluated by averaging the SER of the AWGN channel using the PDF of the fading envelope. To estimate the SER for coherent MPSK signaling over the AWGN channel, one can obtain an approximate expression by employing the nearest neighbor approximation method [32, 34–36].

$$SER_{MPSK} \approx 2Q\left(\frac{d_{min}}{\sqrt{2N_0}}\right) = 2Q\left(\frac{2A \sin \frac{\pi}{M}}{\sqrt{2N_0}}\right) = 2Q\left(\sqrt{2\gamma} \sin\left(\frac{\pi}{M}\right)\right) \quad (25)$$

where A is commonly determined by the signal energy and d_{min} is the minimum distance of the constellation.

The Q-function, represented as $Q(\sqrt{b\gamma}) = \frac{1}{\pi} \int_0^{\frac{\pi}{2}} \exp\left(-\frac{b\gamma}{2} \sin^2 \theta\right) d\theta$, where $b = 2 \sin^2(\pi/M)$, is defined in [4]. By employing the trapezoidal rule to solve for $Q(\sqrt{b\gamma})$, a simplified closed form of (25) is stated as:

$$SER_{MPSK} = \frac{1}{t} \left[\frac{e^{-b\gamma/2}}{2} + \sum_{i=1}^{t-1} e^{-b\gamma/S_i} \right] \quad (26)$$

In this context, t corresponds to the count of summations, where $S_i = 2 \sin^2 \theta_i$ and $\theta_i = \frac{i\pi}{2t}$.

To determine the SER for MPSK in the new system, the SER of an AWGN channel is averaged over the PDF of a Nakagami- m fading channel with N_r receive antennas at a given instantaneous SNR [36].

$$P_{ser} = E[SER_{MPSK}] = \int_0^\infty SER_{MPSK} f_\gamma(\gamma) d\gamma \tag{27}$$

Since $f_\gamma(\gamma) = \left(\frac{m}{\bar{\gamma}}\right)^{mN_r} \frac{\gamma^{mN_r-1}}{\Gamma(mN_r)} \exp\left(-\frac{m\gamma}{\bar{\gamma}}\right)$, $\gamma \geq 0$ for the MRC [37], by substituting this expression in (27), we obtain

$$P_{ser} = \int_0^\infty \frac{1}{t} \left[\frac{e^{-b\gamma/2}}{2} + \sum_{i=1}^{t-1} e^{-b\gamma/S_i} \right] \left(\frac{m}{\bar{\gamma}}\right)^{mN_r} \frac{\gamma^{mN_r-1}}{\Gamma(mN_r)} \exp\left(-\frac{m\gamma}{\bar{\gamma}}\right) d\gamma \tag{28}$$

The convergence of (28) can be achieved by utilizing the property of the Gamma function as provided in [9, 37, 38]. For $\alpha > 0$,

$$\int_0^\infty \gamma^{\alpha-1} e^{-\gamma\lambda} d\gamma = \frac{\Gamma(\alpha)}{\lambda^\alpha} \text{ for } \lambda > 0; \tag{29}$$

Upon solving Eq. (28) with the help of (29), (28) transforms into

$$P_{ser_MRC} = \frac{1}{t} \left[\frac{1}{2} \left(\frac{2m}{b\bar{\gamma} + 2m}\right)^{mN_r} + \sum_{i=1}^{t-1} \left(\frac{mS_i}{b\bar{\gamma} + mS_i}\right)^{mN_r} \right] \tag{30}$$

The SER for the new system can be demonstrated to be

$$SER = \frac{1}{t} \left[\frac{1}{2} \left(\frac{2m}{\widehat{b\bar{\gamma}}_{k,c} + 2m}\right)^{mN_r} + \sum_{i=1}^{t-1} \left(\frac{mS_i}{\widehat{b\bar{\gamma}}_{k,c} + mS_i}\right)^{mN_r} \right] \tag{31}$$

By substituting $\widehat{\gamma}_{k,c}$ with the expressions provided in (12) and (24), results in

$$SER = \frac{1}{t} \left[\frac{1}{2} \left(\frac{2m}{b\epsilon_k \beta_c \bar{\gamma} + 2m}\right)^{mN_r} + \sum_{i=1}^{t-1} \left(\frac{mS_i}{b\epsilon_k \beta_c \bar{\gamma} + mS_i}\right)^{mN_r} \right] \tag{32}$$

Theoretical and simulation results

The study utilizes Monte-Carlo simulations to verify the validity of the decorrelation gain equation derived in (21) and the SER equation derived in (32). Additionally, we demonstrate the performance of the virtual receive diversity system using various antenna configurations for the MPSK modulation scheme.

In the legends of the figures, the labels 'Corr' and 'Decorr' represent the correlated system and the proposed decorrelated(virtual receive diversity) system, respectively. The term 'Sim' corresponds to the results obtained from simulations, while 'Theory' represents outcomes from the analytical framework described in Eq. (32). This study considers fading channels that conform to the Nakagami-m distribution and assumes arbitrary correlation, which is modeled using the Bessel model. The correlation model assumes a linear antenna array with a uniform distribution of the angle of arrival (AoA). The correlation coefficient, denoted by ρ , is expressed as [21].

$$\rho = J_0\left(2\pi \frac{d}{\lambda}\right) \tag{33}$$

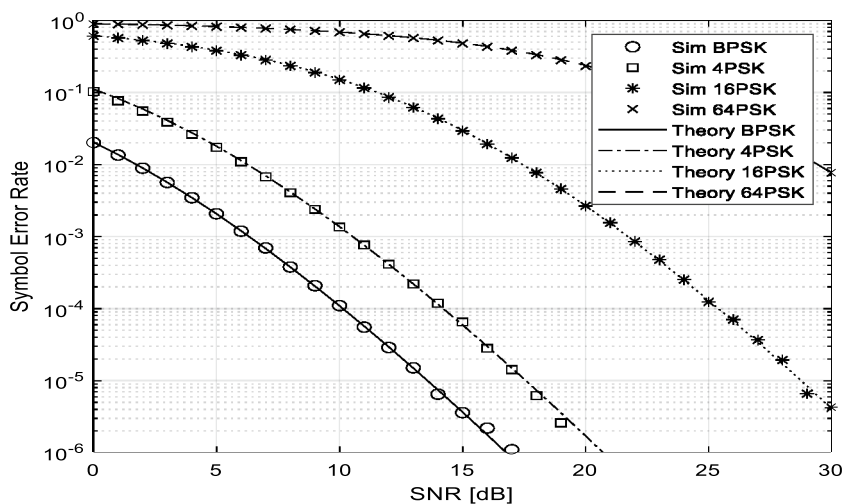


Fig. 2 Comparing simulated and analytical SER for the decorrelator with $m = 1, N_r = 4,$ and $d = 0.2\lambda$

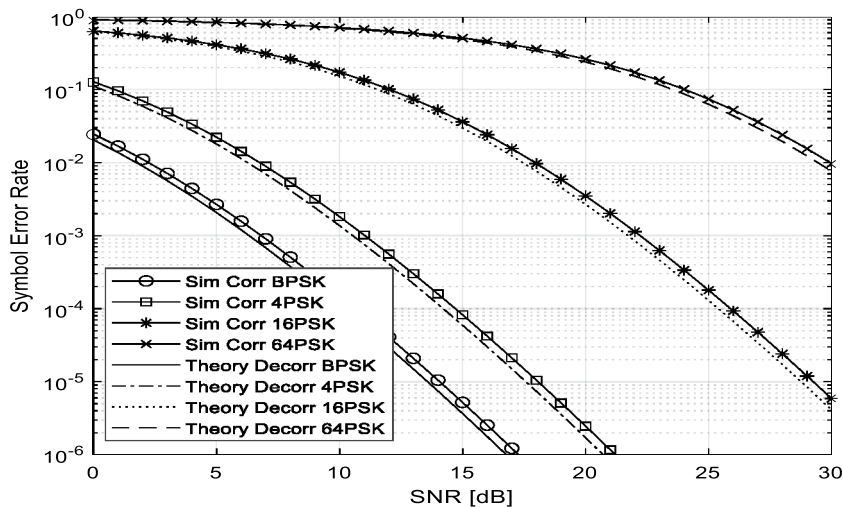


Fig. 3 Comparing SER between correlated and decorrelated systems with $N_r = 4, m = 1,$ and $d = 0.2\lambda$

J_0 corresponds to the Bessel function of the first kind with a zero order, d signifies the separation distance between antennas, and λ symbolizes the wavelength of the carrier signal.

Figure 2. compares the SER performance of BPSK, 4-PSK, 16-PSK, and 64-PSK modulation schemes with a diversity order of four and an antenna separation distance of 0.2λ when $m = 1$. BPSK exhibits the best performance, followed by 4-PSK, 16-PSK, and 64-PSK in terms of SER. For a given SNR, such as 15 dB, the SER values are 3.666×10^{-6} , 5.93×10^{-5} , 2.977×10^{-2} , and 0.236 for BPSK, 4-PSK, 16-PSK, and 64-PSK, respectively. This observation aligns with the well-established fact that the SER performance generally deteriorates as the number of phases and symbols increases. This is due to the higher susceptibility of higher-order M-PSK schemes to noise and phase errors. Consequently, BPSK typically exhibits better SER performance when compared to higher-order M-PSK schemes like 4-PSK, 16-PSK, and 64-PSK.

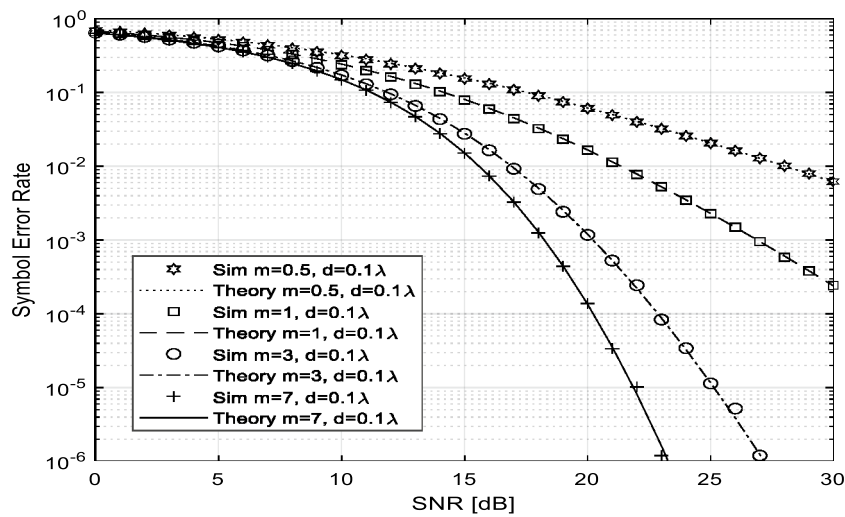


Fig. 4 Analyzing fading parameter’s impact on the SER for the decorrelated system with $N_r = 3$ and $d = 0.1\lambda$

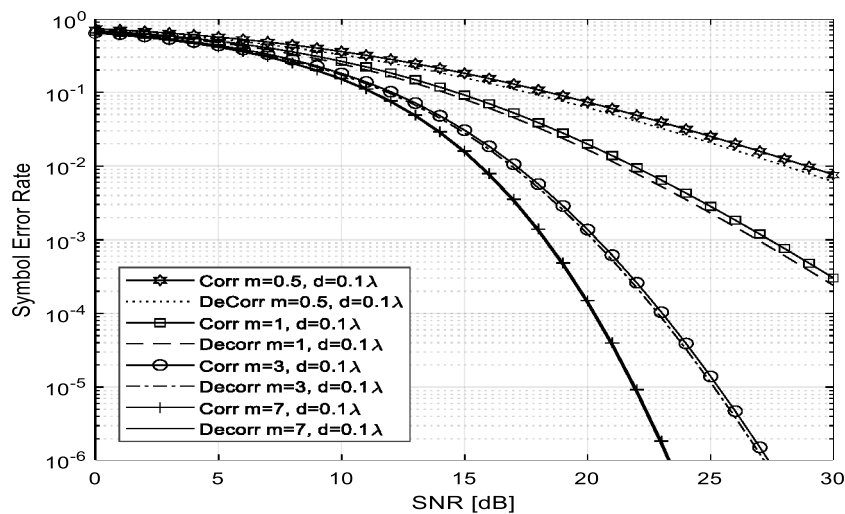


Fig. 5 Comparing SER between correlated and decorrelated systems with varying m , $N_r = 4$, and $d = 0.1\lambda$

In Fig. 3., we demonstrate the performance of the virtual receiver diversity by comparing theoretical results of a correlated system and a virtual receiver diversity system for BPSK, 4-PSK, 16-PSK, and 64-PSK, where $N_r = 4$, $m = 1$, and $d = 0.2\lambda$. It can be deduced that the proposed virtual receiver diversity achieves decorrelation gains of approximately 1 dB for the EGC systems. A greater increase in decorrelation gain implies that a reduced SNR is required to achieve an equivalent SER, suggesting improved performance even in the presence of noise.

Figure 4. illustrates the influence of the fading parameter, m , which characterizes the Nakagami- m distribution, on the error performance of the M-PSK modulation scheme using the proposed virtual receiver diversity decorrelator. The study considered a diversity order of 3 and an antenna spacing equivalent to 0.1 of the wavelength. As anticipated,

increasing m resulted in a decrease in SER, while decreasing m had the opposite effect, at a constant SNR. For instance, at a SNR of 20 dB, the SER values were 0.06164, 0.01662, 1.196×10^{-3} , and 1.351×10^{-4} for 16-PSK when m was set to 0.5, 1, 3, and 7, respectively. This behavior can be attributed to the Nakagami- m distribution becoming more concentrated around its mean value. The increased concentration limits the dispersion of fading effects, resulting in reduced impact on the transmitted signal. Thus, higher values of m indicate a channel less prone to errors, leading to improved SER. Furthermore, it was observed that the simulation and analytical results closely matched for all tested values of fading parameter m , namely 0.5, 1, 3, and 7.

Figure 5. illustrates the effectiveness of the suggested diversity decorrelator by comparing its results with those of a conventional correlated system for 16-PSK. A diversity order of 4 and an antenna spacing of 0.1λ are taken into account. Tests were conducted to examine varying fading parameters: $m = 0.5, 1, 3,$ and 7 . It was observed that the proposed diversity decorrelator achieves decorrelation gains of approximately 1 dB at a SER of 10^{-3} for $m = 1$. However, as the value of m increases, the decorrelation gains decrease. For higher values of m , the decorrelation gains become negligible. This is attributed to less severe fading and fewer rapid fluctuations in the received signal power. As m approaches infinity, the channel experiences no fading.

Figure 6. showcases the effectiveness of the diversity decorrelator in terms of performance. The simulation results are compared for $N_r = 3$, with different antenna spacings. It is anticipated that antennas positioned closer together would exhibit greater signal correlation, leading to a higher SER. This expectation is confirmed by the simulations, as the SER decreases when the antenna spacing changes from $d = 0.1\lambda$ to $d = 0.5\lambda$. Additionally, it is worth noting that the suggested diversity decorrelator achieves approximately 1 dB of decorrelation gain for the EGC combiner systems.

Figure 7 compares the impact of diversity order on the performance of EGC and MRC SER with 16-PSK, with $m = 3$ and $d = 0.2\lambda$. According to the graph, the proposed virtual diversity receiver system achieves equivalent error performance to MRC in

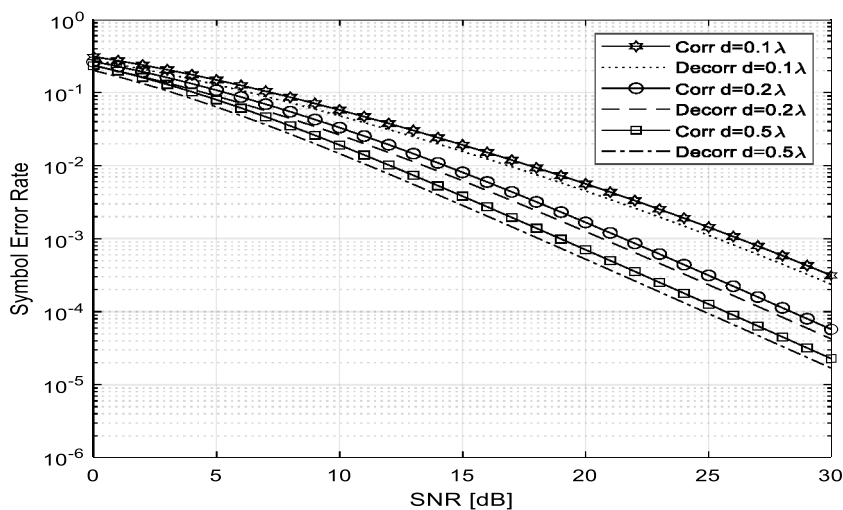


Fig. 6 Comparing SER for correlated and decorrelated EGC, with $N_r = 3$ and $m = 0.5$

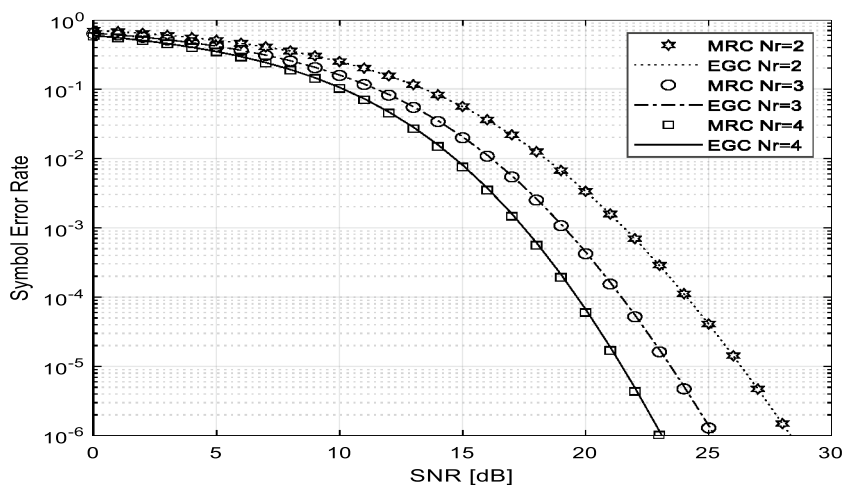


Fig. 7 Comparing SER between EGC and MRC for $m = 3, d = 0.2\lambda$, and $N_r = 2, 3, 4$

correlated systems. This can be explained as follows: In channels with significant fading, EGC combines branches with high noise levels, resulting in a significant penalty compared to MRC. However, in balanced channels with low fading, EGC takes full advantage of combining all the “good” branches, approaching the performance of MRC. This can also be attributed to the fact that as fading severity decreases, the relative weights of MRC approach unity, which are the EGC weights. One key finding is that instead of using the computationally complex MRC combining, EGC can be employed with the diversity decorrelator to achieve similar gains.

Conclusion

A virtual receiver diversity decorrelator that does not require the measurement of signal information from a correlated system has been analyzed for M-PSK signals using coherent EGC reception. The virtual receiver diversity decorrelator achieves decorrelation gains for EGC in channels that follow the Nakagami- m statistical distribution. The decorrelation gain obtained depends on the fading parameter m . Additionally, a decorrelation gain expression is derived for EGC reception in M-PSK correlated signals in channels experiencing fading according to the Nakagami- m distribution. Finally, the decorrelation gain expression derived is integrated into the derived SER expression for EGC to obtain the overall SER expression for the virtual receiver diversity decorrelator. The SER for the virtual receiver diversity decorrelator is validated through Monte Carlo simulation results. The expression results are found to be tightly bound to the simulation results. It is also demonstrated that the performance of EGC approaches the performance of MRC. An important outcome is that the utilization of the computationally complex MRC can be replaced by the implementation of EGC to achieve equivalent benefits, particularly in cases where the diversity decorrelator is engaged. Nevertheless, the developed decorrelator exhibits certain limitations. Owing to correlations between the sum and difference signals, the resultant decorrelated

outputs, referred to as conjoint signals, do not demonstrate complete mutual independence. Thus, the decorrelator solely mitigates the extent of correlation.

Abbreviations

AfDB	African development bank
AoA	Angle of arrival
AWGN	Additive white Gaussian noise
BPSK	Binary phase shift keying
DFT	Discrete fourier transform
FFT	Fast fourier transform
EGC	Equal gain combining
EVD	Eigenvalue decomposition
KLTK	Karhunen-Loeve transformation
M-PSK	M-ary phase-shift keying
MRC	Maximum-ratio combining
PDF	Probability density function
PCA	Principal component analysis
SC	Selection combining
SER	Symbol error rate
SIMO	Single-input multiple-output
SLC	Square law combining
SNR	Signal-to-noise ratio
SSC	Switch and stay combining
UCA	Uniform circular array

Acknowledgements

The authors express their gratitude to their departments for offering research environments and resources that facilitated the execution of this study.

Author contributions

EO: Wrote the original draft, derived the analytical framework, and validated it through Monte Carlo simulations. PA: Developed the initial research idea, supervised the research, oversaw the research process, and coordinated activities among co-authors. JX: Edited and revised the manuscript to improve clarity and accuracy. VO: Critically reviewed the research paper, providing constructive feedback and suggestions that improved the paper. Each author reviewed and endorsed the final version of the manuscript.

Funding

The study received partial funding from the African Development Bank (AfDB) in collaboration with the Kenyan Ministry of Education.

Availability of data and materials

The research findings in this paper are backed by openly accessible data that can be produced through Monte Carlo simulations. Additionally, you can acquire the data by reaching out to the corresponding author.

Code availability

The code can be obtained by contacting the corresponding author upon reasonable request.

Declarations

Ethics approval and consent to participate

Not applicable.

Consent for publication

Not applicable.

Competing interests

The researchers involved in this study assert that they possess no financial or personal interests that could potentially sway the research outcomes or interpretations when publishing the paper.

Received: 15 August 2023 Accepted: 13 September 2023

Published online: 11 October 2023

References

1. Ayeni O, Ojo J, Owolawi P, Ajewole M (2023) Performance comparison of diversity techniques with additive white gaussian channel (awgc) in free space optical communication (fso) under atmospheric turbulence scenario. *Int J Phys Sci* 18(1):12–18. <https://doi.org/10.5897/IJPS2020.4896>
2. Lin J, Poor HV (2020) Optimum combiner for spatially correlated nakagami-m fading channels. *IEEE Trans Wireless Commun* 20(2):771–784. <https://doi.org/10.1109/TWC.2020.3028284>

3. Olutayo A, Cheng J, Holzman J (2020) Performance bounds for diversity receptions over a new fading model with arbitrary branch correlation. *EURASIP J on Wireless Commun Netw*. <https://doi.org/10.1186/s13638-020-01705-5>
4. Rao D (2019) Channel coding techniques for wireless communications. Springer, Singapore. <https://doi.org/10.1007/978-981-15-0561-4>
5. Akuon P, Xu H (2017) Gain of spatial diversity with conjoint signals. *IEEE Africon 2017 Proceedings, Cape Town, South Africa*, 110–114. <https://doi.org/10.1109/AFRCON.2017.8095465>
6. Zhou B, Yang F, Cheng J, et al. (2016) Performance bounds for diversity receptions over arbitrarily correlated nakagami-m fading channels. *IEEE Trans Commun* 15(1):699–713
7. Dwivedi VK, Singh G (2003) Error-rate analysis of the ofdm for correlated nakagami- m fading channel by using maximal-ratio combining diversity. *Int J Microw Wirel Technol* 3(6):717–726. <https://doi.org/10.1017/S175907871000742>
8. Akansu AN, Torun MU (2012) Toeplitz approximation to empirical correlation matrix of asset returns: a signal processing perspective. *IEEE J Selected Topics in Signal Process* 6(4):319–324. <https://doi.org/10.1109/JSTSP.2012.2204724>
9. N, K, (2019) A review of selection combining receivers over correlated rician fading. *Elsevier-Digital Signal Process* 88:1–22
10. Hangani S, Beaulieu NC (2008) On the benefits of decorrelation in dual-branch diversity. *IEEE International Conference on Communications (ICC)*, 4696–4702. <https://doi.org/10.1109/ICC.2008.880>
11. Dong X, Beaulieu NC (2002) Optimal maximal ratio combining with correlated diversity branches. *IEEE Commun Lett* 6:22–24
12. Xu H, Akuon P (2002) A receive decorrelator for a wireless communications system. Patent 2 016 733 215. [Online]. Available: <https://patents.google.com/patent/WO2017001995A1/en>
13. Pan Y, Zhou Y, Liu W, Ni L (2020) A Generalization of Principal Component Analysis. *IEEE Explorer*
14. Li M, Zhang F, Ji Y, Fan W (2022) Virtual antenna array with directional antennas for millimeter-wave channel characterization. *IEEE Trans Antennas Propag* 70(8):6992–7003. <https://doi.org/10.1109/TAP.2022.3161334>
15. Alibakhshikenari M, Virdee B, Mariyanayagam D, al, (2023) Virtual antenna array for reduced energy per bit transmission at sub-5 ghz mobile wireless communication systems. *Elsevier- Alexandria Eng J* 71:439–450
16. Wang Y, Chen X, Liu X (2021) al: Improvement of diversity and capacity of mimo system using scatterer array. *IEEE Trans Antennas Propag* 70(1):789–794. <https://doi.org/10.1109/TAP.2021.3098568>
17. Beaulieu NC (2008) Pre-processor for receiver antenna diversity,. Patent 08 748 200. [Online]. Available: <https://patents.google.com/patent/WO2008144879A1/en>
18. Al-Juboori S, Fernando X (2019) Characterizing a decorrelator for selection combining receivers in nakagami-m fading channels. *AEU - Int J Electron Commun* 106:12–19
19. Fang L, Bi G, Kot AC (2000) New method of performance analysis for diversity reception with correlated rayleigh-fading signals. *IEEE Trans Veh Technol* 49:1807–1812
20. Loyka S, Tellambura C, Kouki A, et al. (2000) New method of performance analysis for diversity reception with correlated rayleigh-fading signals. *IEEE Trans Veh Technol* 49:1807–1812
21. Haghani S, Beaulieu C (2009) On decorrelation in dual-branch diversity systems. *IEEE Trans Commun* 51(7):12–19
22. Karagiannidis G, Zogas D, Kostopoulos S (2003) Performance analysis of triple selection diversity over exponentially correlated nakagami-m fading channels. *IEEE Trans Commun* 51:1245–1248
23. Chen Y, ellambura C, (2004) Distribution functions of selection combiner output in equally correlated rayleigh, rician, and nakagami-m fading channels. *IEEE Trans Commun* 52:1948–1956. <https://doi.org/10.1109/TCOMM.2004.836596>
24. Akuon P, Xu H (2016) Optimal error analysis of receive diversity schemes on arbitrarily correlated rayleigh fading channels. *IET Commun* 10:854–861. <https://doi.org/10.1049/iet-com.2015.0965>
25. Karagiannidis G, Zogas D, Kostopoulos S (2004) Ber performance of dual predetection egc in correlated nakagami-m fading. *IEEE Trans Commun* 52:50–53. <https://doi.org/10.1109/TCOMM.2003.822166>
26. Omosa E, Akuon P, Kalecha V, (2019) Reed-solomon(rs) coding gain on correlated rayleigh fading. (2019) *IEEE Africon*. *IEEE Xplore*. <https://doi.org/10.1109/AFRICON46755.2019.9133926>
27. Zhang F, Ngo K, Yang S, Nosratinia A (2022) Transmit correlation diversity: generalization, new techniques, and improved bounds. *IEEE Trans Inf Theory* 68(6):3841–3869. <https://doi.org/10.1109/TIT.2022.3146523>
28. Aksoy E (2020) *Advances in Array Optimization*. IntechOpen, ILndon. <https://doi.org/10.5772/intechopen.83276>
29. Horn R, Johnson C (2013) *Matrix Analysis*, 2nd edn. Cambridge University Press, Cambridge. <https://doi.org/10.1017/CBO9780511810817>
30. Moon T, Stirling W (2000) *Mathematical methods and algorithms for signal processing*, 1st edn. Prentice-Hall, New Jersey
31. Tsai M, Bashir M, Alouini M (2022) Data combining schemes for a detector array receiver in free-space optical communications. *IEEE Open J Commun Soc* 3:1090–1102. <https://doi.org/10.1109/OJCOMS.2022.3181812>
32. Simon M, Alouini SM (2004) *Digital Commun Over Fading Channels*, 2nd edn. Wiley-IEEE Press, New York
33. García FA, Mora HC, Garzón NO (2022) Improved exact evaluation of equal-gain diversity receivers in rayleigh fading channels. *IEEE Access* 10:26974–26984. <https://doi.org/10.1109/ACCESS.2022.3157752>
34. Al-Anbagi H, Vertat I (2020) Collaborative Network of Ground Stations with a Virtual Platform to Perform Diversity Combining. *IEEE Explorer*. <https://doi.org/10.1109/AE54730.2022.9920037>
35. Rugini L (2020) Sep bounds for mpsk with low snr. *IEEE Commun Lett* 24(11):2473–2477. <https://doi.org/10.1109/LCOMM.2020.3012837>
36. Jia Y, Wang Z, Yu J, Kam P (2023) A new approach to deriving closed-form bit error probability expressions of mpsk signals. *IEEE Trans Commun*. <https://doi.org/10.1109/TCOMM.2023.32802187>

37. Adachia F, Boonkajay A (2019) Analysis of maximal-ratio transmit and combining spatial diversity. *IEICE Commun Exp* 8(5):153–159. <https://doi.org/10.1587/comex.2019XBL0015>
38. Laforgia A, Natalini P (2013) Exponential, gamma and polygamma functions: simple proofs of classical and new inequalities. *Elsevier-J Math Anal Appl* 407(2):495–504. <https://doi.org/10.1016/j.jmaa.2013.05.045>

Publisher's Note

Springer Nature remains neutral with regard to jurisdictional claims in published maps and institutional affiliations.

Submit your manuscript to a SpringerOpen[®] journal and benefit from:

- ▶ Convenient online submission
- ▶ Rigorous peer review
- ▶ Open access: articles freely available online
- ▶ High visibility within the field
- ▶ Retaining the copyright to your article

Submit your next manuscript at ▶ [springeropen.com](https://www.springeropen.com)
